

# The influence of joint properties in modelling jointed rock masses

Influence des propriétés des diaclases sur la modélisation des masses rocheuses diaclasées  
Der Einfluß von Spaltbrucheigenschaften auf die Modellbildung von geklüfteten Felsmassen

NICK BARTON, Norwegian Geotechnical Institute, Oslo, Norway

**ABSTRACT:** Prediction of likely response to excavation, and production of final designs for the rock reinforcement, require realistic descriptions of the components of rock mass behaviour. This article explores some of the methods that have proved reasonably successful in describing and modelling rock joints and rock masses, despite the complexities involved. Index testing of rock joints and rock mass characterisation, including geophysical methods, are the essential activities in preparation for two- and three-dimensional distinct element modelling. Recent improvements are described.

**RESUME:** La prévision de la réponse vraisemblable d'un massif rocheux lors de la réalisation d'une excavation, ainsi que le dimensionnement des renforcements nécessaires, nécessitent une description réaliste du comportement des composants de ce massif. Cet article explore quelques unes des méthodes qui se sont montrées raisonnablement satisfaisantes pour la description et la modélisation des massifs rocheux et de leurs joints, en dépit de la complexité que cela suppose. Les essais sur joints et la caractérisation du massif (y compris par les méthodes géophysiques) sont les éléments essentiels préalables à une modélisation en deux ou trois dimensions par éléments discontinus. Des développements récents sont décrits.

**ZUSAMMENFASSUNG:** Die Vorhersage der wahrscheinlichen Gebirgsreaktion auf das Auffahren von Untertageräumen und das Design von Felsverstärkungen verlangt die wirklichkeitsnahe Beschreibung der einzelnen Komponenten des Felsverhaltens. Dieser Artikel beschreibt einige Methoden, welche trotz ihrer Komplexität, erfolgreich zur Klüft- und Felsmodellierung und Beschreibung angewandt werden. Das Indextesten von Klüften und die Gebirgsklassifizierung, geophysikalische Methoden eingeschlossen, sind wesentliche Bestandteile in der Vorbereitungsphase von zwei und dreidimensionalen bestimmten Elemente Simulationen. Neuere Entwicklungen werden beschrieben.

## 1 INTRODUCTION

This article explores some of the methods which appear to be having some success in realistic modelling and design for jointed rock masses. Key techniques are joint index testing, rock mass characterisation, seismic measurements and distinct element modelling. At NGI, these methods can be represented by the following basic symbols: JRC, JCS,  $\phi_r$ ,  $Q$ ,  $V_p$ , UDEC and 3DEC. The first three are the index parameters for the joint sets of concern (Barton and Bandis, 1990). The  $Q$ -values give estimates for rock mass moduli and rock reinforcement, following Grimstad and Barton, 1993. The two- and three-dimensional distinct element models UDEC and 3DEC conceived by Cundall and refined by Itasca Inc. provide the final essential link to reality.

Spatial variability within the rock mass which is reflected to some extent by the statistics for JRC, JCS,  $\phi_r$  and  $Q$ , is further described by the seismic measurements which provide a means of extrapolation between mapping locations (i.e., exposures or drill core). In its optimal form (cross-hole seismic tomography), it gives detailed information that can be approximately correlated to  $Q$ -values and to deformation modulus, using recent developments.

## 2 SHEAR BEHAVIOUR OF ROCK JOINTS

Direct shear tests of rough-walled tension fractures developed in weak model materials, that were performed many years ago when the author was a student, indicated the importance of both the surface roughness and the uniaxial strength ( $\sigma_c$ ) of the rock. The empirical relation for peak shear strength given in Equation 1 was essentially the forerunner of the subsequent JRC-JCS or Barton-Bandis model, where the joint roughness coefficient

(JRC) was equal to 20 for these rough tension fractures. The joint wall strength (JCS) was equal to  $\sigma_c$  (the unconfined compression strength).

$$\tau = \sigma_n \tan \left[ 20 \log \left( \frac{\sigma_c}{\sigma_n} \right) + 30^\circ \right] \quad (1)$$

The original form of Equation 1 is therefore perfectly consistent with today's equation:

$$\tau = \sigma_n \tan \left[ \text{JRC} \log \left( \frac{\text{JCS}}{\sigma_n} \right) + \phi_r \right] \quad (2)$$

Equation 1 represents the three limiting values of the three input parameters, i.e.,

- JRC = 20 (roughest possible joint without actual steps)
- JCS =  $\sigma_c$  (least possible weathering grade, i.e., fresh fracture)
- $\phi_r = \phi_0$  (fresh unweathered fracture with basic friction angles in the range  $28\frac{1}{2}$  to  $31\frac{1}{2}^\circ$ ).

Bandis et al., 1981, 1983 and Barton et al., 1985, have subsequently shown how these three index parameters JRC, JCS and  $\phi_r$  can be used for modelling both the shear-dilation and normal closure behaviour of rock joints with estimation of physical and hydraulic joint aperture, and with due account of scale effects and shear reversals, etc.

Figure 1 illustrates the first version of the constitutive model for shear and dilation behaviour, which was subsequently coded by Itasca for use in UDEC-BB (Christianson, 1985, personal communication) and improved by NGI and Itasca (Gutierrez, 1995; Christianson, 1995, personal communication) for use in an improved version UDEC-BB.

Although different degrees of joint weathering and mineral

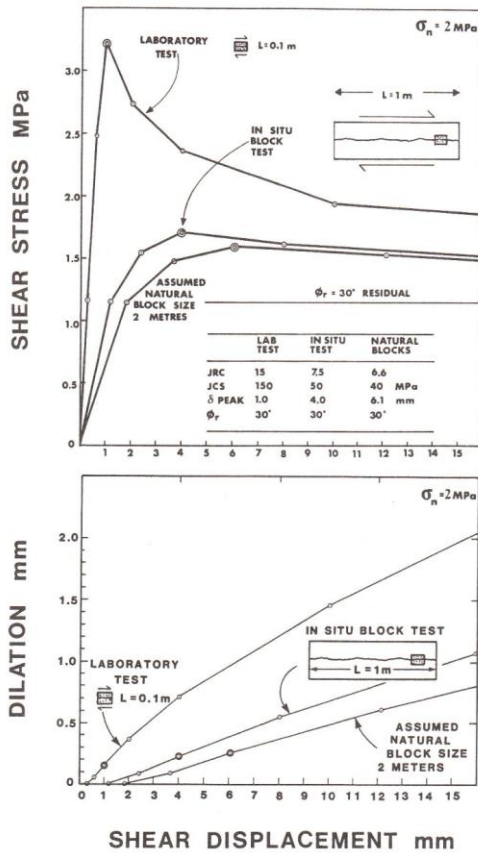


Figure 1. Constitutive model of stress-displacement and dilation-displacement behaviour of rock joints of different size. (Barton, 1982)

coatings can be tackled by the JRC-JCS model, clay-filled discontinuities cannot be treated, and alternative index tests (or direct shear testing) will be needed. The alternative solution is provided by the parameters  $J_r$  (joint roughness number) and  $J_a$  (joint alteration number) in the Q-system (Barton et al., 1974). Figure 2 shows histograms for  $J_r$  and  $J_a$  (the central pair of parameters). It will be noted that there are three categories of  $J_a$ , namely: unfilled, thin fills and thick fills.

Appropriate description of the mineralogy of the filling ( $J_a$ ) and appropriate use of the range of  $J_r$  values (or  $J_r = 1.0$  in the case of fillings with no rock-to-rock wall contact) provides a conservative estimate of the frictional strength through the simple equation:

$$\tau = \sigma_n \left( \frac{J_r}{J_a} \right) \quad (3)$$

Figure 3 illustrates the above forms of shear strength estimation graphically. Further recent evidence for the validity of Equation 3 as a rough indicator of frictional strength is provided by numerous in situ direct shear tests performed at a major dam site in Asia.

Table 1 shows the range of  $J_r$  and  $J_a$  values mapped at various

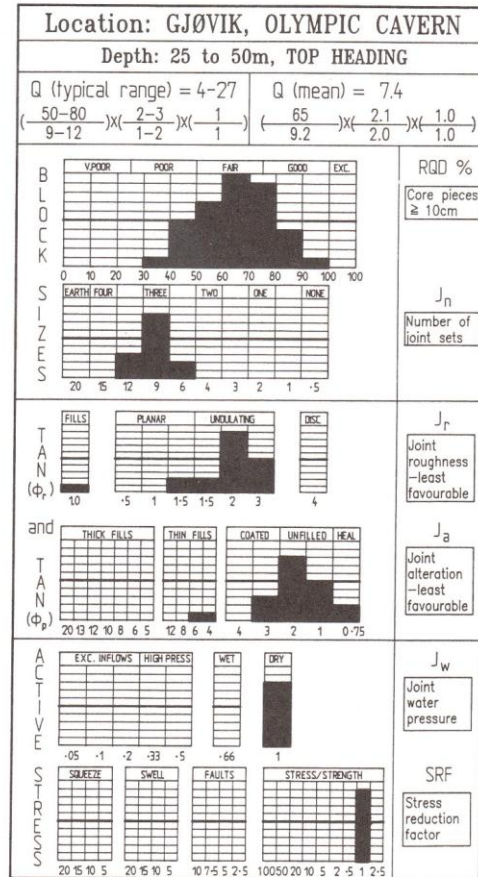


Figure 2. Recording of Q-parameters from which  $J_r/J_a$  values can be estimated for filled discontinuities.

Table 1. Ratio  $J_r/J_a$  from the Q-system as a means of classifying the friction coefficient of intercalations.

Roughness ( $J_r$ )	Filling ( $J_a$ )	rough	smooth	no rock wall contact	
		planar	undulating		
		1.5	2.0	1.0	
THIN FILLS	sandy	4.0	0.38	0.50	N/A
	stiff clay	6.0	0.25	0.33	N/A
	soft clay	8.0	0.19	0.25	N/A
THICK FILLS	silty clay	5.0	N/A	N/A	0.20
	rock & clay	6.0	N/A	N/A	0.17
	rock & soft clay	8.0	N/A	N/A	0.13

exploratory adit sites by the author. The 135 in situ direct shear tests performed in these adits showed a general range of friction coefficients ( $\tan^{-1} \tau/\sigma_n$ ) of 0.18 to 0.38 and design values of

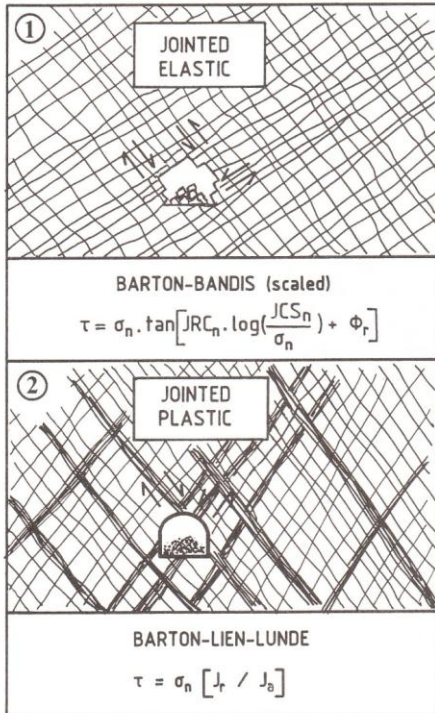


Figure 3. Empirical shear strength estimation for two major categories of rock mass.

0.23 to 0.28. Very thin intercalations showed 0.45, and the extreme range was 0.14 to 0.49. Good correspondence with  $J_r/J_b$  values was indicated.

The advantages of the JRC, JCS,  $J_r$  and  $J_b$  empirical methods of shear strength estimation is that the associated index test methods such as tilt tests and Schmidt hammer tests (or experienced judgement) can each be performed cheaply and often give a good indication of statistical variation. (The necessary index tests are described in detail by Barton and Choubey, 1977 and their suggested presentation for design studies by Barton et al, 1992.)

### 3 ROCK MASS DEFORMABILITY

Deformation modes for rock masses include closure or opening of the joints, shear and dilation (if non-planar surfaces), elastic and non-elastic deformation of the matrix (rock blocks) and complex interactions of all these processes. Since joint hydraulic apertures and general hydraulic connectivity can each be strongly affected by all the above modes, it is clear that simplification is required for allowing reasonable levels of discussion.

Figure 4 is designed to illustrate firstly how the normal deformation and shear deformation components of the constituent joints may affect the overall deformability of different rock masses, under simple uniaxial loading. The normal behaviour of the joints is described by Bandis' hyperbolic formulation, details of which are given by Bandis et al., 1983.

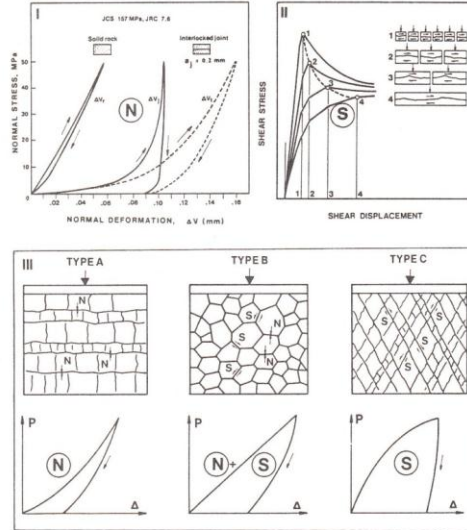


Figure 4. Normal (N) and shear (S) components of joint deformation determine the general form of stress-strain curves for loading tests on rock masses. (Barton, 1985; Bandis et al., 1981; 1983)

The concave (N) component and the convex (S) component are each dominant, or combine with each other, as the case may be. (Types A, C and B respectively). Uniaxial (strain) loading in simple UDEC-BB distinct element models of the same problems are shown in Figure 5.

Despite the uniaxial loading with no lateral strain, the Type C rock mass shows larger overall deformation and of course joint shearing. Peak stresses were also higher in this model.

Physical model studies reported by Barton and Bandis (1982) have indicated higher shear resistance for the jointed assemblies of blocks that had the smallest block sizes. This finding is shown schematically in Figure 6, where models with 4000, 1000 or 250 blocks were studied in biaxial shear. Reduced JRC and JCS values have to be used for the larger block sizes (i.e.,  $JRC_n$  and  $JCS_n$  for block sizes  $L_n$ ).

The two equations given below show how JRC and JCS given in Equation 2 can be scaled down to allow for the lower shear resistance expected at in situ block size.

$$JRC_n = JRC_0 \left( \frac{L_n}{L_0} \right)^{-0.02 JRC_0} \quad (4)$$

$$JCS_n = JCS_0 \left( \frac{L_n}{L_0} \right)^{-0.03 JRC_0} \quad (5)$$

Despite the potential for scale effects connected with block size, in which the smaller blocks may give higher ultimate shear resistance (for equal joint roughness), there is nevertheless a general experience that the deformation modulus of more heavily jointed rock masses is lower than for massive rock masses.

Figure 7, which is an idealised UDEC study of tunnelling in assemblages of 250 to 10,000 blocks using Mohr Coulomb joint parameters (and no built-in joint strength scale effect), shows, as expected, much larger disturbed zones (and deformation) as

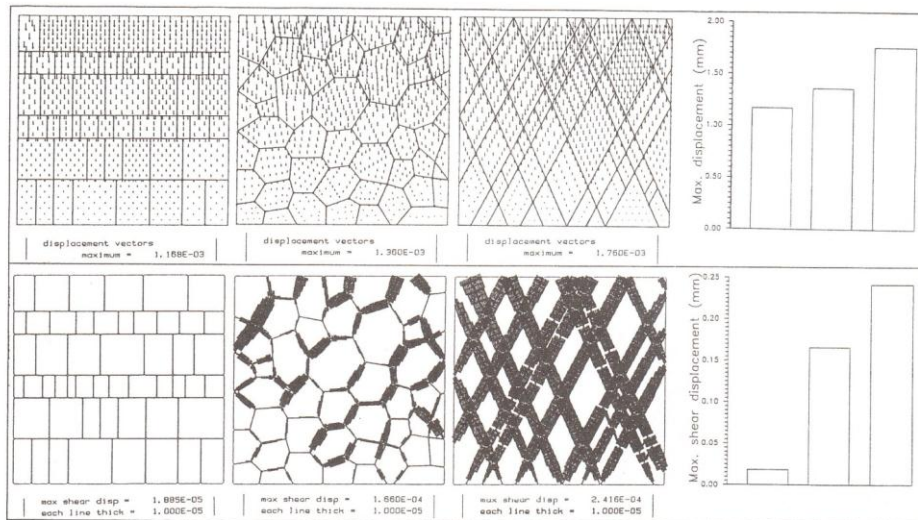


Figure 5. Uniaxial strain loading of three hypothetical rock masses with a 2D UDEC-BB model. (Chryssanthakis et al., 1991)

block size reduces. Figure 8 gives the distributions of joint shearing caused by numerical tunnelling in what is a highly anisotropic stress field ( $\sigma_v = 20$  MPa,  $\sigma_h = 5$  MPa). The deformability of the closely jointed model is clearly by far the highest of the cases studied, with or without tunnel support measures.

Physical models and UDEC models that were driven to a stage of complete tunnel failure showed shear band formation (block rotation) when the block size was sufficiently small compared to the excavation dimensions or loaded boundary dimensions (Shen and Barton, in preparation).

#### 4 ROCK MASS DEFORMABILITY FROM ROCK MASS CLASSIFICATION

It is reasonably certain that the idealised rock mass depicted as Model No. 4 (Figure 7) would (in the real world) have reduced rock mass quality (RMR or Q), reduced deformation modulus (M) and reduced seismic P-wave velocity ( $V_p$ ), as compared to the more massive cases with less rock blocks. In reality there might also be reduced joint roughness or even slickensiding (i.e.,  $J_r = 0.5$ ) and mineralisation (i.e.,  $J_a = 4$ ) (i.e., low JRC, JCS and  $\phi_p$ ) in the case of the rock mass with small block sizes. The above differences in behaviour would be accentuated by the combination of lower deformation modulus and lower shear resistance.

The Q-system of rock mass classification (Barton et al., 1974) is designed to provide greater levels of rock reinforcement and tunnel support in such cases. The fact that the Q-value can vary from 0.001 to 1000 is also a reflection of the enormous range of rock mass deformation moduli (i.e., 0.05 to 50 GPa) and shear strengths (i.e., 0.1 to 20 MPa) that may be encountered, and which may have an accumulative effect on the need for rock reinforcement in the case of tunnelling.

The Q-value of a rock mass is built up from an assessment of relative block size ( $RQD/J_n$ ), inter-block shear strength ( $J_r/J_a$ ) and active stress ( $J_w/SRF$ ); it therefore has close parallels to the processes demonstrated in Figure 8.

It is therefore logical that the wide range of rock reinforce-

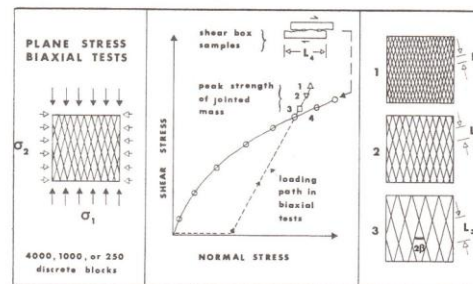


Figure 6. Schematic of physical model tests of fractured rock, indicating block size dependence. (Barton and Bandis, 1982)

ment solutions shown in Figure 9 should also have some relationship with the deformation modulus of the particular rock mass. The same could be said of the Bieniawski (1989) RMR-value, which has an approximate relationship to the Q-value.

Correlations between the RMR-value and the Q-value show significant trends but quite wide scatter, particularly for lower qualities of rock. This is partly due to the absence of the SRF term in the RMR method. Nevertheless, because of the significant sets of data on rock mass deformation modulus in the literature related to the two methods, it is convenient to find a workable correlation between Q and RMR.

In Figure 10, data on rock mass deformation moduli (M) reported by Bieniawski (1978) and Serafim and Pereira (1983) are reproduced, together with these authors' linear and non-linear relationships between M and RMR. On the same figure a suggested correlation between RMR and Q is given, based on the following approximation:

$$RMR \approx 15 \log Q + 50 \quad (6)$$

On the basis of this Q rating scale, the approximation

$$M \approx 10 Q^{\frac{1}{3}} \quad (\text{GPa}) \quad (7)$$

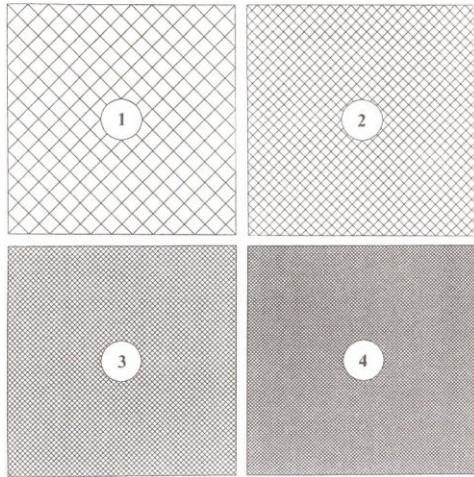


Figure 7. Idealised UDEC models of tunnels within 2D assemblies of 250 to 10,000 blocks. (Shen and Barton, in preparation)

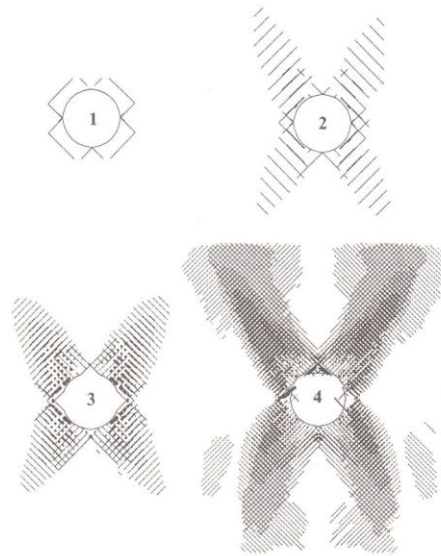


Figure 8. Extent of joint shearing zones caused by widely different block sizes. (Shen and Barton, in preparation)

is proposed for estimating the mean value of rock mass deformation modulus.

The dotted curve in Figure 10 shows good correlation with reported results and extends into the region of low rock qualities, very close to the Serafim and Pereira (1983) relation.

Equation 7 is also shown within a larger set of higher deformation modulus data as the non-linear curve in Figure 11. For fair, good and very good rock qualities, it provides a very similar estimate of modulus to that recommended earlier ( $M = 25 \log Q$ , Barton, 1983), a correlation that has been used successfully in earlier verification studies with UDEC-BB.

## 5 GEOPHYSICAL CLASSIFICATION OF ROCK MASSES

In many countries with deep surface weathering and soil cover, the use of seismic refraction, cross-hole seismic or step frequency radar measurements, may be the only way to extrapolate

rock mass characterisation data between mapped rock exposures or between available cored drill holes. Unless drill holes are sufficiently deep (and close), there may also be uncertainty concerning the rock mass quality at tunnel depth since the refraction measurements have limited penetration. There are other complications connected with the influence of stress level (i.e., depth) and rock density and porosity effects, each of which will influence the interpretation of seismic velocity and its relation to rock mass quality.

International interest in potential correlations between rock mass quality, rock mass deformation modulus and seismic velocity has been considerable for many years, and various correlations have been suggested, including well known correlations with RQD. The advent of cross-hole seismic tomography in the last ten years or so, and concerns with nuclear waste

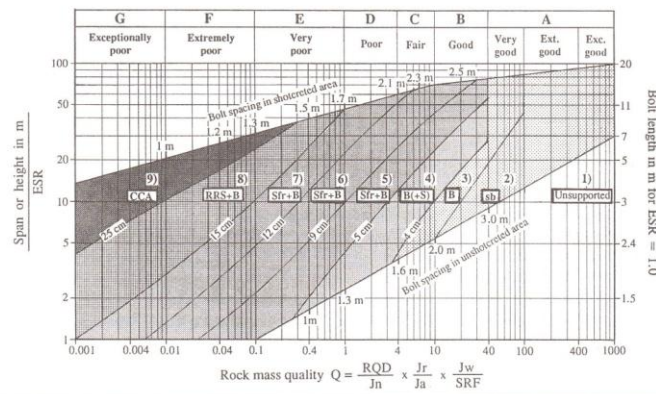


Figure 9. The Q-system of classification and reinforcement selection. (Grimstad and Barton, 1993)

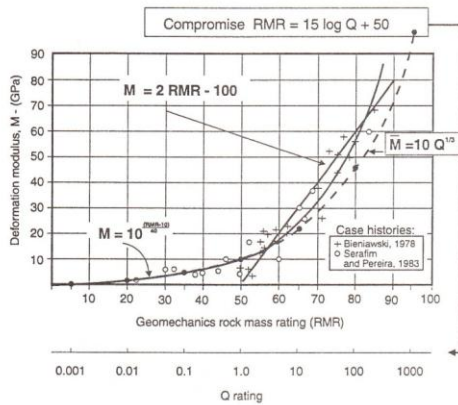


Figure 10. Approximations to deformation modulus based on RMR and Q; covering the lower ranges of rock qualities.

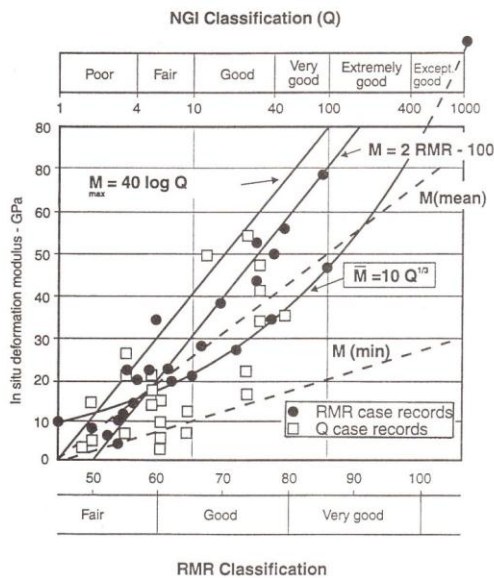


Figure 11. Approximation to deformation modulus covering the higher ranges of rock qualities.

repository design has heightened this interest.

In 1991, NGI performed cross-hole seismic measurements at the site for Norway's Olympic rock cavern at Gjøvik. Results (redrawn for clarity of reproduction) are presented in Figure 12. These measurements which are described more fully in Barton et al. (1994), gave the opportunity for detailed correlation between Q-logging of the core and the adjacent velocity calculations.

The general trend observed at this site and for hard rocks at other shallow sites (i.e., 25 to 50m depth) in other countries is as follows:

$$V_p \approx \log Q + 3.5 \quad (\text{km/s}) \quad (8)$$

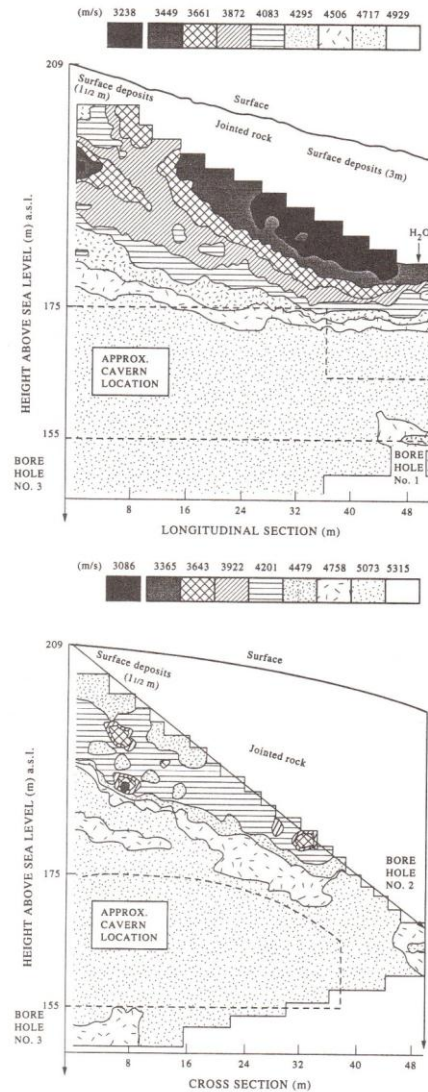


Figure 12. Cross-hole seismic tomography at the Olympic cavern site, Gjøvik.

i.e.,  $V_p \approx 3.5$  km/s for  $Q = 1$ ,  $V_p \approx 4.5$  km/s for  $Q = 10$ , etc.

Additional study of results from other sites around the world, including weak and porous rocks such as chalk, sandstone and tuff, and deep locations accessed by cross-hole tomography has resulted in the suggested correlations between quality, velocity and modulus given in Figure 13.

Essential features of the seismic correlation chart are:

- 1) correction for increased stress or depth (causing increase in velocity and deformation modulus),
- 2) correction for increased porosity ( $n\%$ ) or reduced uniaxial compression strength ( $\sigma_c$ ) (causing reductions in velocity and deformation modulus).

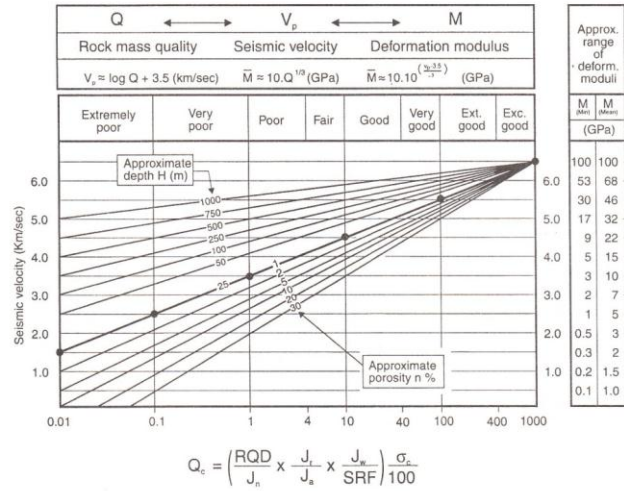


Figure 13. Rock mass quality, seismic velocity and deformation modulus correlations for design.

The compression strength correction is applied by "normalising" the Q-values to a nominal hard rock compression strength value of 100 MPa.

$$Q_c = Q \times \frac{\sigma_c}{100} \quad (9)$$

This correction is to allow the Q<sub>c</sub> value to reflect the influence of rock compression strength on seismic velocity.

The standard Q-value is reduced by SRF when the ratio of rock strength to major principal stress (σ<sub>c</sub>/σ<sub>1</sub>) implies rock failure problems and need for increased rock reinforcement. Although V<sub>p</sub> and M values will be expected to reduce in the excavation disturbed zone (EDZ) (as shown in Figure 14), the correlations given in Figure 13 should be applied with caution in the EDZ around a tunnel.

An example will be used to illustrate how to use the seismic correlation chart (Figure 13):

Assume Q = 4 and σ<sub>c</sub> = 25 MPa, therefore Q<sub>c</sub> = 1

Assume H = 250m and n% = 5%

The latter are expected to cause approximately (+) 1.2 and (-) 0.6 km/s change in seismic velocity for Q<sub>c</sub> = 1, compared to the shallow (25m) nominal value. Therefore V<sub>p</sub> ≈ 4.0 km/s and the mean deformation modulus (at 250m depth) ≈ 15 GPa.

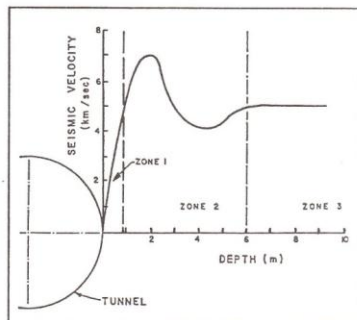


Figure 14. Seismic measurements in circular tunnels showing effect of stress concentration. (Plichon, 1980)

These correlations will usually be applied in reverse order, i.e., by measuring V<sub>p</sub> at depth H, with estimated n% and σ<sub>c</sub> (MPa) values, an approximate Q-value could be selected for preliminary assessment of rock support needs. For design purposes the seismic measurement would allow the rock mass deformation modulus to be estimated, prior to in situ measurement or direct classification of core.

## 6 PRESENTATION OF JOINT AND ROCK MASS DATA

The geotechnical logging chart prepared as a Lotus spreadsheet in Figure 15 shows how the previously described joint and rock mass logging and index test data can be assembled for rapid reference. Each chart might represent the statistics from several core boxes, from several kilometres of surface or tunnel mapping or from a completed project.

The logging statistics shown in Figure 15 have data arranged as in Table 2. This means that:

- the upper third of the chart gives geometrical properties of the rock mass (for building the numerical models),
- the middle third of the chart gives joint strength and roughness (for strength and deformability input to the models), and
- the lower third of the chart gives approximate ranges of permeability, rock strength and major stress (for defining boundary conditions in the models).

## 7 UTILISATION OF LOGGED DATA IN UDEC-BB AND 3DEC

Utilisation of joint and rock mass logging data (Figure 15) for numerical distinct element modelling is illustrated by an example UDEC-BB model in Figure 16. The inset below the figure shows the joint index data for laboratory scale values of JRC, JCS and φ<sub>r</sub>. [A large scale joint roughness (i) value of 6° was also assessed at this site.]

The deformation moduli of 20, 30 and 40 GPa at depths of 0-45m, 45-65m and 65-125m shown in Figure 16 were estimated from Q-logging and from evaluation of the seismic measurements. It will be noted from Figure 12 that the seismic tomography shows V<sub>p</sub> values in the range 4 to 5 km/s in the

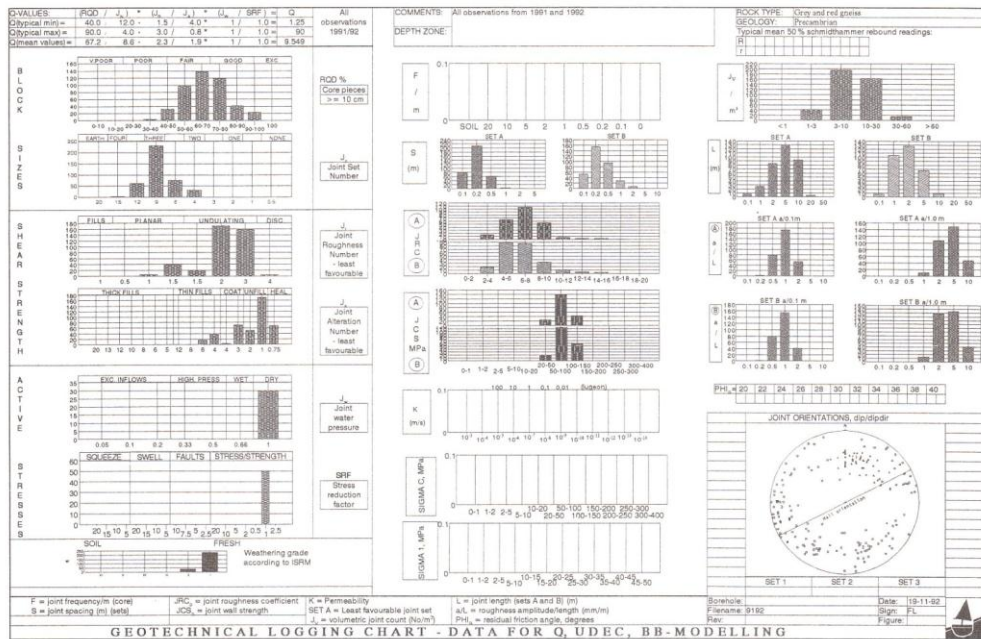


Figure 15. Geotechnical logging chart; data for Gjøvik Olympic cavern of 62m span. (from Barton et al., 1994)

Table 2. The parameters represented in the geotechnical logging chart.

I ROCK MASS STRUCTURE				
1	RQD	Deere et al., 1967	block size	Q
2	$J_n$	= joint set number		Q
3	F	= joint frequency (per metre)		
4	$J_v$	= volumetric joint count (Palmström, 1982)		
5	S	= joint spacing (in metres)		
6	L	= joint length (in metres)		
7	w	= weathering grade (ISRM, 1978)		
8	$\alpha/B$	= dip/dip direction of joints (Schmidt diagram)		
II JOINT CHARACTER				
9	$J_r$	= joint roughness number	shear strength	Q
10	$J_a$	= joint alteration number		Q
11	JRC	= joint roughness coefficient		
12	a/L	= roughness amplitude of asperities per unit length (mm/m)		
13	JCS	= joint wall compressive strength		
14	$\phi_r$	= residual friction angle		
15	r,R	= Schmidt rebound values for joint and rock surfaces		
III WATER, STRESS, STRENGTH				
16	$J_w$	= joint water reduction factor	active stress	Q
17	SRF	= stress reduction factor		Q
18	K	= rock mass permeability (m/s)		
19	$\sigma_c$	= compressive strength		
20	$\sigma_1$	= major principal stress		

neighbourhood of the cavern arch. Since the uniaxial strength ( $\sigma_c$ ) was 60-90 MPa for the gneissic rocks, and the porosity was negligible, correlation with mapped Q-values generally in the range 2 to 30 is seen to agree with the seismic correlation in Figure 13.

Anisotropy of  $V_p$  in the main body of the cavern, i.e., 4717m/s in the longitudinal section sub-parallel to the minimum horizontal stress and 5073m/s in the cross-section sub-parallel to the major horizontal stress which was some 1.5 to 2 MPa higher, is also broadly consistent with the stress or depth correction given in Figure 13.

Joint and rock mass data obtained from logging some 1.5 km of core and from surface mapping in the portal areas was the basis for the UDEC-BB model of a twin lane road tunnel shown in Figures 17 and 18. This modelling was initially performed to check the rock bolt loading as a verification of the Q-system design.

The hydraulic apertures shown in Figure 17 (middle) show stress-induced reduction with depth (maximum value = 44  $\mu\text{m}$ ). The maximum stress caused by excavation was 8 MPa. The displacements, joint shearing and bolt loading shown in Figure 18 have maximum values of 3.9mm, 2.6mm and 6.9 tons respectively.

Besides bolt representation, fibre reinforced shotcrete representation in UDEC and UDEC-BB is now a reality following recent Itasca and NGI developments made by Lorig (personal communication, 1995). Use of special structural elements means that even the stability of uneven shotcreted excavation profiles can be studied. An extreme example of overbreak is shown in Figure 19.

The importance of correct representation of jointing, in particular the dilation component, i.e., Figure 1, bottom, is now even more important, if modelled bolting (Lorig, 1985) and modelled shotcrete support are each to be realistically loaded. The idealised example shown in Figure 20 (Chryssanthakis,

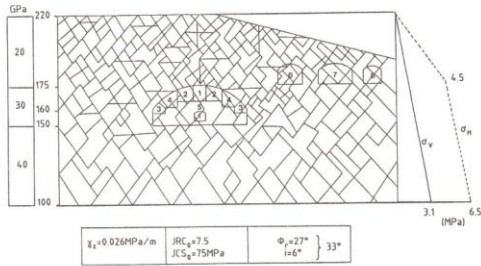


Figure 16. Joint and rock mass input data for a UDEC-BB model of the Gjøvik Olympic cavern. (Barton et al., 1994)

personal communication 1995) illustrates a square opening with shotcrete in both cases, but with two rock bolts supporting an unstable wedge in one case. The loading of the shotcrete (axial or shear forces, moments or adhesion) without the bolts (or if inadequate bolting were installed) is obviously strongly dependent on as correct description of the joint properties JRC, JCS and  $\phi_r$  as possible.

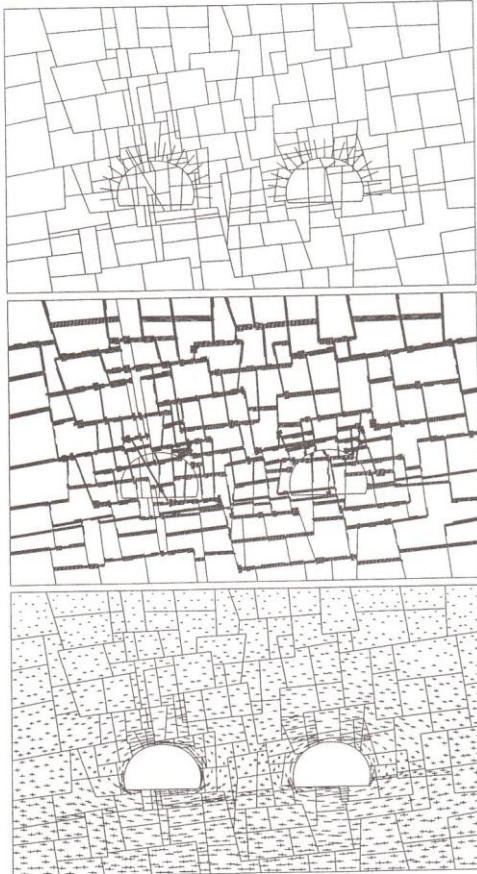


Figure 17. Block geometry, bolting, hydraulic apertures and induced stresses caused by excavation of twin road tunnels. (Backer, 1993)

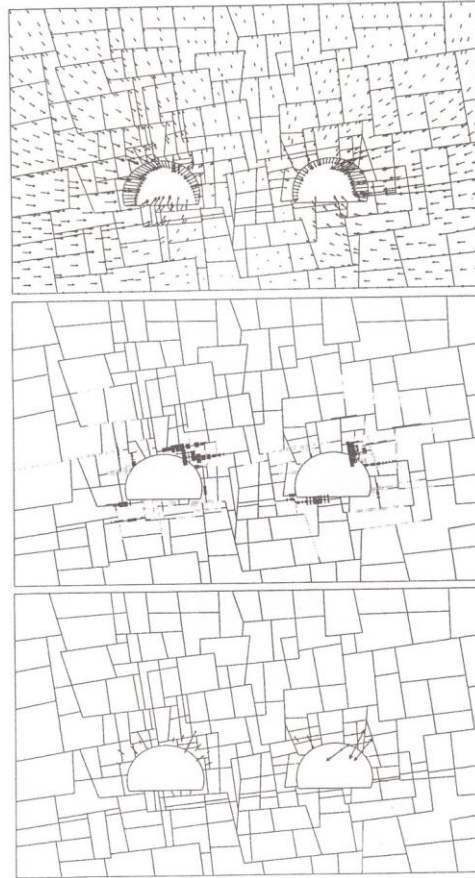


Figure 18. Displacements, joint shearing and bolt loading caused by excavation of twin road tunnels. (Backer, 1993)

The development of 3DEC by Cundall (1988) and Hart et al. (1988) has opened new vistas for realistic numerical modelling of rock masses. Although some refinements have yet to be added, the ability to represent in approximate terms the statistics of joint orientation and persistence as illustrated in Figure 21 is of inestimable value. Jointed block diagrams such as those illustrated, can be "drilled" through, "pilot tunnelled", or rotated to

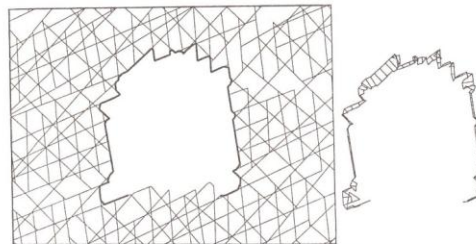


Figure 19. Modelling fibre reinforced shotcrete S(fr) in 2D discrete element models. (Lorig, 1995)

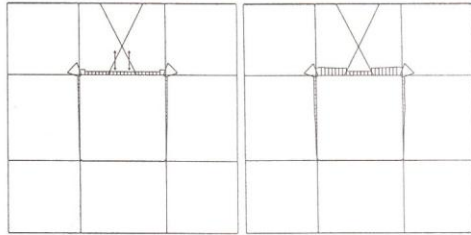


Figure 20. Axial loading of  $S(fr)$  in an idealised UDEC model of a square opening with and without bolts. (Chryssanthakis, 1995)

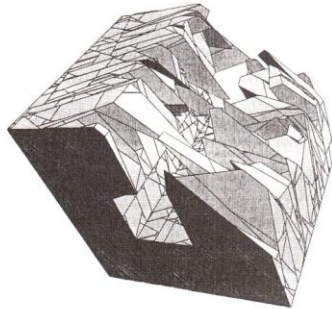


Figure 21. Three-dimensional visualisation of jointing with 3DEC and "pilot tunnelling" investigations. (Shen, 1994)

find optimal orientations both for realistic 2D modelling with UDEC (if this choice was available) or for full blown 3D stress and deformation analyses. The rock mechanics community are in debt to Cundall and his Itasca colleagues vision of the way forward for modelling jointed rock.

## 8 CONCLUSIONS

1. This keynote article has taken a personal, biased look at some of the techniques that are available for modelling joints and jointed rock masses.
2. The techniques utilised include index tests for describing the empirically based JRC and JCS parameters of individual joints or joint sets. The Q-system and RMR system of rock mass classification are utilised in an attempt to provide realistic estimates of rock mass deformation moduli.
3. Linkages between the rock mass quality Q-value, the seismic velocity  $V_p$  and the rock mass deformation modulus  $M$  have been established, with approximate allowance for the effect of depth, and for the porosity and uniaxial compression strength of the rock concerned.
4. The assembly of necessary index and classification data into a well organised format that is user friendly and economic in terms of volume (cellulose friendly?) has been demonstrated.
5. Utilisation of the joint and rock mass data in the distinct element models UDEC-BB and 3DEC has been illustrated by examples, including the use of rock bolting and fibre reinforced shotcrete sub-routines. The correct loading of these important components of modern rock reinforcement is dependent on the joint and rock mass description that precedes these analyses.

## 9 REFERENCES

- Backer, L., 1993, Personal communication.  
 Bandis, S., A. Lumsden and N. Barton, 1981, "Experimental studies of scale effects on the shear behaviour of rock joints", *Int. J. of Rock*

- Mech. Min. Sci. and Geomech. Abstr.* 18, pp. 1-21.  
 Bandis, S., A.C. Lumsden and N. Barton, 1983, "Fundamentals of Rock Joint Deformation", *Int. J. Rock Mech. Min. Sci. and Geomech. Abstr.* Vol 20, No. 6, pp. 249-268.  
 Barton, N., R. Lien and J. Lunde, 1974, "Engineering classification of rockmasses for the design of tunnel support", *Rock Mechanics*, Vol. 6, No. 4, pp. 189-236.  
 Barton, N. and V. Choubey, 1977, "The shear strength of rock joints in theory and practice", *Rock Mechanics*, Springer, Vienna, No. 1/2, pp. 1-54. Also NGI-Publ. 119, 1978.  
 Barton, N., 1982, "Modelling rock joint behaviour from *in situ* block tests: Implications for nuclear waste repository design", Office of Nuclear Waste Isolation, Columbus, OH, 96 p., ONWI-308, September 1982.  
 Barton, N. and S. Bandis, 1982, "Effects of Block Size on the Shear Behaviour of Jointed Rock", Keynote Lecture, 23rd U.S. Symposium on Rock Mechanics, Berkeley, California.  
 Barton, N., 1983, "Application of Q-System and Index Tests to Estimate Shear Strength and Deformability of Rockmasses", Panel Report, Int. Symp. on Engineering Geology and Underground Construction, Lisbon, Portugal.  
 Barton, N., 1985, "Deformation Phenomena in Jointed Rock", 8th Laurits Bjerrum Memorial Lecture, Oslo. Publ. in *Geotechnique*, Vol. 36, No. 2, pp. 147-167, (1986).  
 Barton, N., S. Bandis and K. Bakhtar, 1985, "Strength, Deformation and Conductivity Coupling of Rock Joints", *Int. J. Rock Mech. & Min. Sci. & Geomech. Abstr.* Vol. 22, No. 3, pp. 121-140.  
 Barton, N. and S.C. Bandis, 1990, "Review of predictive capabilities of JRC-JCS model in engineering practice", International Symposium on Rock Joints. Loen 1990. Proceedings, pp. 603-610, 1990.  
 Barton, N., F. Løset, A. Smallwood, G. Vik, C. Rawlings, P. Chryssanthakis, H. Hansteen and T. Ireland, 1992, "Geotechnical Core Characterisation for the UK Radioactive Waste Repository Design". 1992 Proc. of ISRM Symp. EUROCK, Chester, UK.  
 Barton, N., T.L. By, P. Chryssanthakis, L. Tunbridge, J. Kristiansen, F. Løset, R.K. Bhasin, H. Westerdahl, G. Vik, 1994, "Predicted and Measured Performance of the 62m span Norwegian Olympic Ice Hockey Cavern at Gjøvik", *Int. J. Rock Mech. Min. Sci. & Geomech. Abstr.*, Vol. 31, No. 6, pp. 617-641. Pergamon.  
 Bieniawski, Z.T., 1978, "Determining Rock Mass Deformability: Experience from Case Histories", *Int. J. Rock Mech. Min. Sci. Geomech. Abstr.*, Vol. 15, pp. 237-247.  
 Bieniawski, Z.T., 1989, *Engineering Rock Mass Classifications: A Complete Manual for Engineers and Geologists in Mining, Civil and Petroleum Engineering*, J. Wiley, 251 p.  
 Chryssanthakis, P., K. Monsen and N. Barton, 1991, "Tunnelling in jointed rock simulated in a computer" (In Norwegian). *Tunneller og Undergrunnsanlegg, 1989-1991*, NTNf, Oslo, pp. 23-28.  
 Cundall, P.A., 1988, "Formation of a Three-Dimensional Distinct Element Model - Part I: A Scheme to Detect and Represent Contacts in a System Composed of Many Polyhedral Blocks.", *Int. J. Rock Mech. Min. Sci. & Geomech. Abstr.*, 25, pp. 107-116.  
 Grimstad, E. and N. Barton, 1993, "Updating of the Q-System for NMT", Proceedings of the International Symposium on Sprayed Concrete - Modern Use of Wet Mix Sprayed Concrete for Underground Support, Fagernes, 1993, (Eds Kompen, Opsahl and Berg. Norwegian Concrete Association, Oslo.  
 Gutierrez, M., 1995, Personal communication.  
 Hart, R., P. Cundall and J. Lemos, 1988, "Formation of a Three-Dimensional Distinct Element Model - Part II: Mechanical Calculation for Motion and Interaction of a System Composed of Many Polyhedral Blocks." *Int. J. Rock Mech. Min. Sci. & Geomech. Abstr.*, 25, pp. 117-126.  
 ISRM, 1978, "Suggested methods for the quantitative description of discontinuities in rock masses", (Coordinator, Barton, N.) *Int. J. Rock Mech. Sci. and Geomech. Abstr.*, Vol. 15, pp. 319-368, Pergamon.  
 Lorig, L.J., 1985, "A simple numerical representation of fully-bonded passive rock reinforcement for hard rocks." *Computers and Geotechnics* 1, pp 79-97  
 Lorig, L.J., 1995 Personal communication.  
 Palmström, A., 1982, "The Volumetric Joint Count - A Useful and Simple Measure of the Degree of Rock Mass Jointing", in Proc. 4th Cong. Int. Assoc. of Engineering Geology, New Delhi, India, Vol. 5, Theme 2, pp. V.221-V.228.  
 Plichon, J.N., 1980: Measurements of the thickness of the decompressed zone in an excavation under high overburden cover. in *Analysis of Tunnel Stability by the Convergence-Confinement Method*, Underground space, 4, vol. 6 pp. 361-402.  
 Serafim, J.L. and J.P. Pereira, 1983, "Considerations of the Geomechanics Classification of Bieniawski". *Proc. Int. Symp. Eng. Geol. Underground Constr.*, LNEC, Lisbon, 1983, vol. 1, pp. II.33-II.42.  
 Shen, B. and Barton, N., in preparation, "The disturbed zone around tunnels in jointed rock masses".